Implementing 4D XCAT phantom for 4D radiotherapy research

Significance and Innovation

Various techniques have been developed for motion management of moving targets in radiotherapy. Implementing a realistic and flexible 4D digital human phantom is of great importance for evaluating and developing 4D imaging and treatment techniques.

Introduction

As new technique for respiratory motion management in radiotherapy [1] is flourishing day by day, we need some sort of motion phantom that can validate, evaluate and optimise the best resource available in the clinic. Respiratory model of 4D XCAT digital phantom is based on respiratory mechanics and analysis of state of the art respiratory gated CT data which is flexible and parameterised that includes the ability to model the lung nodules of any given size, shape, contrast and location inside the lungs [2].

Methods and Materials

An integrated computer program was developed in Matlab (R2009a, the Mathworks Inc., Natick, MA) to facilitate the characterization and implementation of the 4D XCAT phantom. Fig. 1 shows the workflow of the program that consists of the following essential functions: (1) Generating 4D XCAT images, which was achieved by running the core XCAT programs developed by Segars *et al.* [2] (2) Reviewing 4D XCAT images. (3) Generating composite images from 4D XCAT, including maximum intensity projection (MIP), average intensity projection (AIP), and minimum intensity projection (MinIP). (4) Motion tracking for a selected region of interest (ROI), such as diaphragm, lesion, body surface, etc. (5) Converting XCAT phantom images from the raw binary format into DICOM format. (6) Analyzing clinically acquired 4DCT and Real-time Position Management (RPM) signal. Major characteristics of the 4D XCAT phantom that are relevant to 4D RT applications were studied as described below: (1) Dependence of lesion motion on lesion location. (2) Dependence of lesion motion on diaphragm motion. (3) Dependence of lesion motion on lesion size. (4) Customization of phantom motion. A real patient's RPM data was inputted as the diaphragm profile for XCAT generation. Measured diaphragm motion from the XCAT images were then compared to the inputted RPM signal.

End-to-end test of the implementation of the 4D XCAT was performed. In this example, 10 frames were generated over a whole respiratory cycle. MIP and AIP images were generated using all 10 frames, converted to DICOM format, and imported into Eclipse treatment planning system for contouring and planning. Internal target volume (ITV) was delineated in the MIP, and organs at risk (OARs) including lung, heart, spinal cord, chest wall, etc., were delineated in the AIP. Planning target volume (PTV) was created by adding a 5 mm margin to the ITV. A lung SBRT plan was created on the AIP using co-planar 3D conformal technique. The prescription dose of 48 Gy in 4 fractions was designed to provide coverage for 95% of PTV. Dose constraints to OARs were adapted from Radiation Therapy Oncology Group (RTOG) 0915 protocol. Analytical Anisotropic Algorithm (AAA) was used for dose calculation.

Results

There is small mean difference of 1.2 mm in motion amplitude between manual and automatic tracking methods (Fig. 2). The study of dependency of lesion location on its excursion shows that the farther the lesion located from diaphragm, the lesser the excursion it has (Fig. 3). There is no size dependency on lesion motion excursion (Fig. 4). The 4D XCAT phantom can closely reproduce irregular breathing profile of RPM respiratory signal with the mean difference in motion amplitude between the inputted and the measured motion profile was 1.4 mm (Fig. 5). The 4D radiotherapy treatment plan generated based on 4D XCAT image shows that the plan is comparable to clinical ones (Fig. 6).

Conclusion

An integrated computer program has been developed to generate, review, analyze, process, and export the 4D XCAT images for 4D RT research. Major characteristics of the 4D XCAT phantom have been studied and an end-to-end test from XCAT image generation to treatment planning has been successfully performed. These preliminary results demonstrated that we have established a robust workflow to implement the 4D XCAT phantom for 4D RT research.

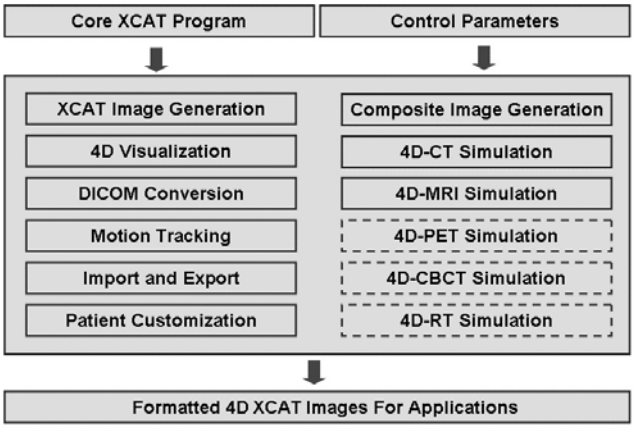

Fig. 1 Workflow of the integrated computer program.

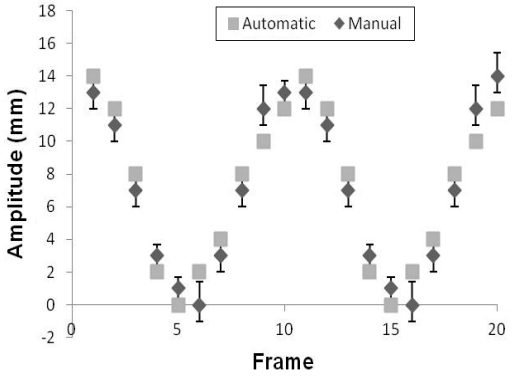

Fig. 3 Comparision of motion trajectories measured automatically and manually.

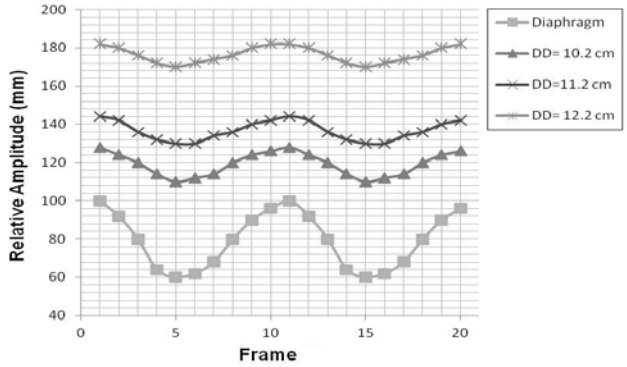

Fig. 3 Cranial-caudal motion trajectories of the lesion at different locations and of the diaphragm. (DD means the distance from the lesion to diaphragm.)

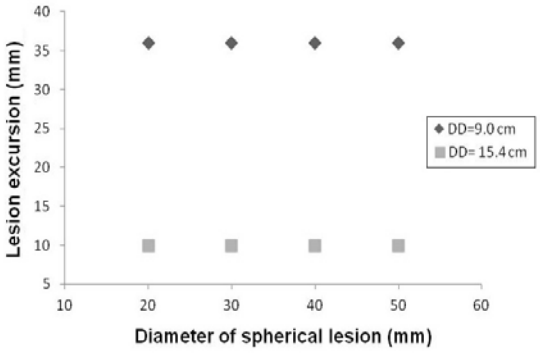

Fig. 4 Dependency of cranial-caudal motion of the lesion on lesion size.

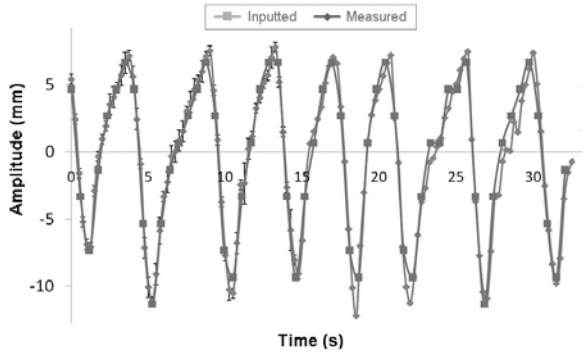

Fig. 5 Comparision between the measued and the inputted motion trajectories.

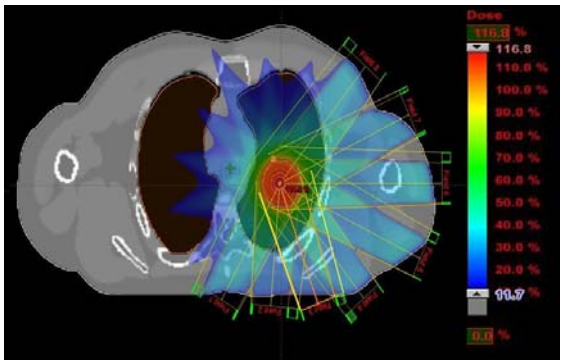

Fig. 6 Beam arrangement and dose distribution of a lung SBRT plan created on the XCAT phantom.

References:

1. Keall PJ, et al. Med Phys. 2006; 33:3874-3900.
2. Segars WP, et al. Med. Phys. 2010;37(9):4902-4915.